geoconvention
Virtual Event
September 21-23
2020
CSPG • CSEG • CWLS • GAC • MAC • IAH

To decluster or not to decluster? Implications for seismic hazard analysis in induced seismicity

Mauricio Reyes Canales[1] and Mirko van der Baan[1]

[1]Dept. of Physics, Univ. of Alberta, Edmonton, AB, T6G 2G7, Canada.

Summary

We investigate if separating mainshocks and aftershocks using a temporal declustering approach leads to more accurate hazard assessments, particularly for large magnitude events. We apply a simulation method based on the Epistemic-Type Aftershock Sequence (ETAS) to generate mainshock (declustered) and complete (non-declustered) synthetic earthquake catalogs. The mainshocks follow a Poissonian distribution. The ETAS model ensures the aftershocks are both non-Poissonian and strongly non-stationary. When the b-value of the mainshock catalog is considerably smaller than the b-value of the complete catalog, declustering leads to more accurate estimates of the b-value for the largest magnitude events. Thus, declustering is only recommended in catalogs with a large number of earthquakes or in catalogs where the b-values of the mainshocks are significantly different than the b -values of the complete catalog. Finally, we analyze a recent case of induced seismicity: Oklahoma, USA, where the complete (non-declustered) catalog displays a kink in the magnitude-frequency distribution. Declustering removes this kink, leading to a more accurate b-value estimation for the largest magnitude events.

Theory

The Epistemic-Type Aftershock Sequence (ETAS) model (Ogata, 1988) is a self-exciting point process in which every event can produce offspring of events. The model includes the background activity and the aftershock events produced by a parent event (either a background or an aftershock event). The rate λ at time t is given by (Ogata, 1988):

$$\lambda = \mu + \sum_{t_i<t} g(t - t_i), \text{ (eq.1)}$$

where μ is the background constant seismicity rate, which is assumed to follow a temporal Poisson distribution. On the other hand, $g(t - t_i)$ is the rate of activity at time t triggered by an event m_i at time t_i, and is given by:

$$g(t - t_i) = K \frac{e^{\alpha(m_i - M_{min})}}{(t - t_i + c)^p}, \text{ (eq. 2)}$$

where M_{min} is the minimum magnitude considered. The parameters K, α, c and p are constants common to all aftershock sequences. The parameter K is related to the productivity of the earthquake, α measures the efficiency of an earthquake to generate aftershocks, c and p are parameters that described the rate of decay given by the modified Omori's law (Utsu, 1961) The second term in eq. 1 represents the addition of all the rates of earthquakes from the aftershock activity, at a given time t. We use the Gutenberg-Richter (GR) parameters, a- and b- values, of declustered catalogs to obtain the rate of the mainshocks, instead of using the background seismicity from the ETAS process.

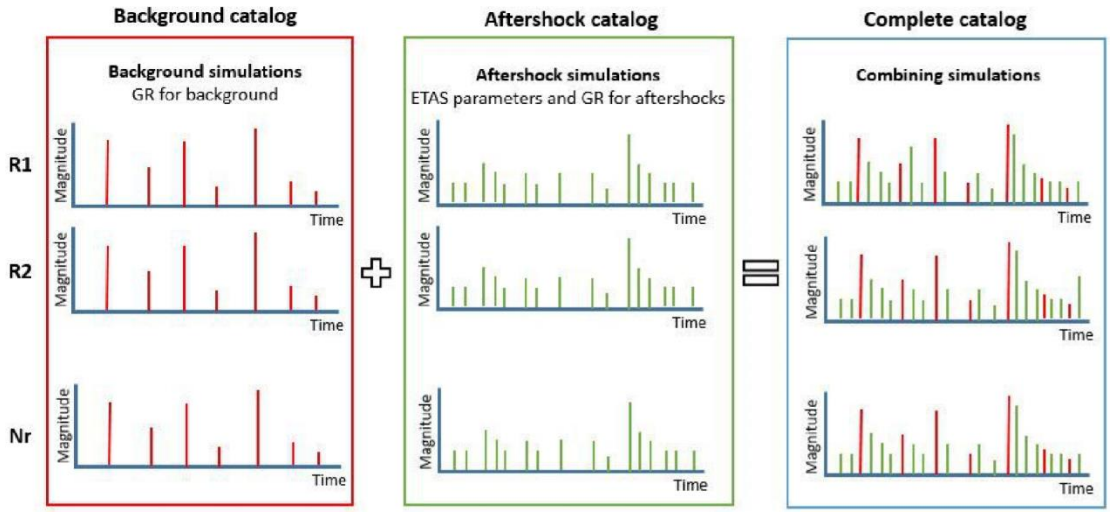

Figure 1. *Sketch of the branching process used to simulate synthetic earthquakes, following the ETAS methodology. The background catalog (Left) is generated assuming a Poisson process. For each background earthquake, a sequence of aftershocks (Center) is generated, following the Epistemic-type process. The complete catalog contains all events (Right).*

We use the branching process method to simulate the ETAS model and generate synthetic earthquake catalogs. This method consists of two main steps: (1) generation of the synthetic earthquake catalogs for the background seismicity, assuming a Poisson process (μ eq.1); (2) generation of the aftershock catalog, where each background event result in a cascade of triggering-direct aftershocks, aftershocks of those aftershocks, etc. For the generation of synthetic mainshock earthquakes (declustered catalog), we apply Monte Carlo simulations as described by Reyes Canales and van der Baan (2019). For the aftershock simulations, a non-stationary Poisson simulation is applied to each event, as described by Zhuang and Touati (2015). The combination of both mainshocks and aftershocks results in the complete (non-declustered) catalog. Figure 1 shows a sketch of the branching process used to simulate synthetic earthquakes methodology. The branching process method allows the use of different b-values for the mainshock and aftershock sequences, which seems to be the case in some observed earthquake catalogs. From the synthetic earthquake catalogs, we can calculate statistical quantities that are relevant for the study of the hazard analysis: (1) the mean annual rate of exceedance $m_{\lambda exc}(m \geq m_j)$ for a magnitude level; (2) the annual rate of exceedance $\lambda_{GR,exc}(m \geq m_j)$ from mean $\hat{a}$-and $\hat{b}$-values; and (3) the probability $P[N = n;\ t_a, t_b]$ of n occurrences in a time interval $\Delta t = [t_a, t_b]$, also from mean $\hat{a}$-and $\hat{b}$-values.

Application to a recent case of induced seismicity: Oklahoma, USA

The recent increase, peak, and decline of the seismic activity in Oklahoma has been one of the most studied cases of induced seismicity worldwide (Ellsworth, 2013; Langenbruch and Zoback 2016; Van der Baan and Calixto, 2017). The seismic activity in Oklahoma has been associated with large volumes of salt-water injection in the Arbuckle formation (Van der Baan and Calixto, 2017). In this study, we use the declustered and non-declustered earthquake catalogs for the 2017 Central and Eastern U.S. short-term seismic hazard model (Petersen et al., 2017). From this catalog, we take the seismicity in Oklahoma between January 2009 and December 2016.

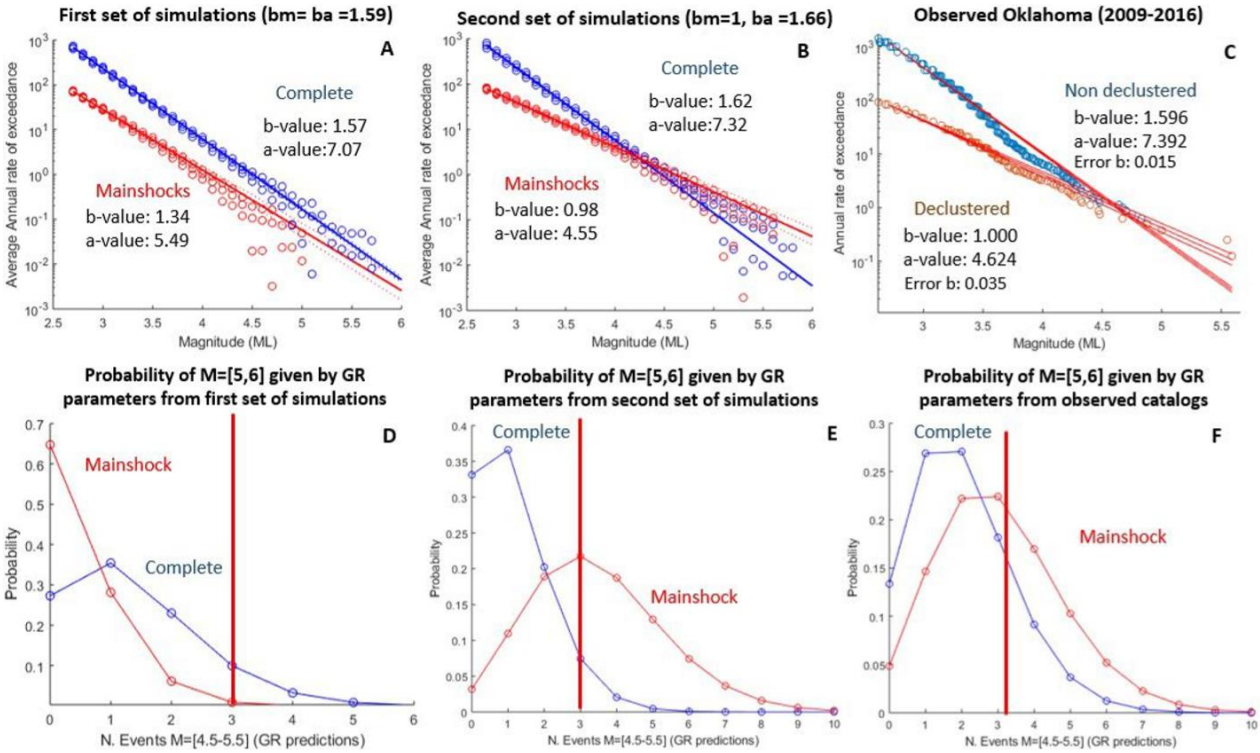

Figure 2. *First row: (A) and (B) show the mean annual rate of exceedance (dotted curves) from the synthetic catalogs and annual rate of exceedance from the mean GR parameters (continuous curves). We consider the same b-value for the mainshock and aftershock events (A), or different b-values for the mainshock and aftershock sequences (B). The upper and lower dashed curves are the mean annual rates ± standard deviation. (C) Estimation of the GR parameters in Oklahoma for declustered and non-declustered catalogs. Second row: Probability of n occurrences in the magnitude range $m = [5.0; 6.0)$, in a 8-year period, given by the complete and mainshock catalogs from (D) the mean GR parameters from the first set ($b_m = b_a = 1.59$), (E) the mean GR parameters from the second set ($b_m = 1.0$ and $b_a = 1.66$) and (F) the GR parameters from the observed seismicity. The number of earthquakes in Oklahoma with local magnitude larger than $m \geq 5$ is $n = 3$ (red vertical lines).*

We apply the ETAS branching process simulation to the Oklahoma data, in order to assess the impact of including or excluding aftershock sequences in the hazard analysis. For the first simulation approach, we assume that the b-values of the mainshock and aftershock sequences are equal to the b-value of the complete catalog, $b_m = b_a = b_c = 1.59$, see figure 2 (C). We set $a_m = 6.60$ for the mainshock sequence. For the second simulation approach, we assume that the a-value and b -values of the background sequence are identical to the a-value and b-value of the observed declustered catalog (mainshock), that is $a_m = 4.60$ and $b_m = 1.0$. On the other hand, for the b-value of the aftershock sequence, we estimate $b_a = 1.66$, which is obtained by applying Maximum Likelihood (MLM) estimations to the residual aftershock sequence resulting from the declustering methodology. We use MLM for the estimation of ETAS parameters (Ogata, 1998). The estimated ETAS parameters for the induced seismicity in Oklahoma are: $c = 0.0204$, $p = 0.8780$, $\alpha = 1.36$, and $K = 1.70$. The central dotted curves in 2 (A) and (B) represent the mean annual rate of exceedance for the complete (blue) and mainshock catalogs (red), estimated by counting events with magnitudes $m \geq m_j$ in the simulated samples. The upper and

lower dotted curves are the mean annual rate of exceedance plus or minus the standard deviation. The central continuous curves the annual rate of exceedance from the mean GR parameters, $\hat{a}$- and $\hat{b}$-values, for complete and mainshock catalogs, estimated from the simulations. The upper and lower dashed curves represent the upper and lower annual rate of exceedance curves plus or minus the standard deviation of mean GR parameters. The second row of figure 2 shows the probability of n occurrences in the magnitude range $m = [5.0;\ 6.0)$, given by the sets of simulations and observed seismicity. When $b_m = b_a = 1.59$, the most likely number of events are $n = 0$ and $n = 1$, given the mean GR parameters of the simulated mainshock and complete catalogs, respectively. When $b_m = 1.0$ and $b_a = 1.66$, the most likely number of events are $n = 3$ and $n = 1$, given the mean GR parameters of the simulated mainshock and complete catalogs, respectively. Finally, using the GR parameters of the observed seismicity, the most likely number of events are $n = 3$ and $n = 2$ given the GR parameters of the mainshock catalog and complete catalog, respectively. 3 earthquakes with local magnitude $m \geq 5$ in Oklahoma occurred between 2009 and 2016 (Petersen et al., 2017). Figure 2 thus shows that the declustering is advisable for a more representative hazard assessment in Oklahoma because the b-value of the aftershocks and mainshocks is different, leading to a non-linear magnitude-frequency distribution.

Conclusions

If mainshocks and aftershocks are characterized by different b-values, declustering leads to improved hazard assessments, since it allows for better estimation of magnitude-frequency distribution of the largest events. Conversely, if mainshocks and aftershocks have similar b-values then declustering is inadmissible since it eliminates larger events that contribute to the long-term hazard. Assuming Poissonian distributions in hazard predictions does not lead to inaccurate long-term hazard predictions. Short-term hazard due to aftershocks is however better estimated by evaluating appropriate non-stationary models such as the ETAS process.

Acknowledgements

The authors would like to thank the sponsors of the Microseismic Industry Consortium for financial support.

References

Ellsworth, W. (2013). Injection-Induced Earthquakes. Science, 341(July), 1–8.

Langenbruch, C., & Zoback, M. D. (2016). How will induced seismicity in Oklahoma respond to decreased saltwater injection rates? Science Advances, 3(8), 1–10.

Ogata, Y. (1988). Statistical models for earthquake occurrences and residual analysis for point processes. Journal of the American Statistical Association, 83(401), 9–27.

Ogata, Y. (1998). Space-time point-process models for earthquake occurrences. Annals of the Institute of Statistical Mathematics, 50(2), 379–402

Petersen, M., Mueller, C. S., Moschetti, M. P., Hoover, S. M., Rukstales, K. S.,703 McNamara, D. E., ... Cochran, E. S. (2017). 2017 one-year seismic hazard forecast for the central and eastern United States from induced and natural earthquakes. Seismological Research Letters, 88(3), 772–783.

Reyes Canales, M., & Van der Baan, M. (2019). Including Non-stationary Magnitude-Frequency distributions in Probabilistic Seismic Hazard Analysis. Pure and App. Geophysics, 176(6), 2299–2319.

Utsu, T. (1961). Statistical study on the occurrence of aftershocks. Geophys. Mag.,723 30, 521–605.

Van der Baan, M., & Calixto, F. (2017). Human-induced seismicity and large-scale hydrocarbon production in the USA and Canada. Geochemistry Geophysics730 Geosystems, 18, 2467–2485.

Zhuang, J., & Touati, S. (2015). Theme V - Models and Techniques for Analyzing Seismicity Stochastic simulation of earthquake catalogs. Community Online Resource for Statistical Seismicity Analysis, 1–34.